ISSN 0965-5441, Petroleum Chemistry, 2020, Vol. 60, No. 8, pp. 937–941. © Pleiades Publishing, Ltd., 2020.
Russian Text © The Author(s), 2020, published in Sovremennye Molekulyarnye Sita, 2020.

A Catalyst System Based on Copper(II) Bromide Supported on Zeolite HY with a Hierarchical Pore Structure in Benzyl Butyl Ether Synthesis

A. R. Bayguzina[a, *], **L. I. Gallyamova**[a], **M. R. Agliullin**[a], **and R. I. Khusnutdinov**[a]

[a] *Institute of Petroleum Chemistry and Catalysis, Russian Academy of Sciences, Ufa, Republic of Bashkortostan, 450075 Russia*

**e-mail: bayguzina2014@gmail.com*

Received February 12, 2020; revised March 13, 2020; accepted April 10, 2020

Abstract—Novel catalyst systems based on $CuBr_2$ supported on zeolite HY with a hierarchical pore structure have been proposed for benzyl butyl ether synthesis by the intermolecular dehydration of benzyl and butyl alcohols. It has been shown that catalyst systems with a $CuBr_2$ content of ~10 wt % provide a benzyl butyl ether yield of ~95% at 150°C.

Keywords: benzyl butyl ether, intermolecular dehydration, benzyl alcohol, *n*-butyl alcohol, copper(II) bromide, micro–meso–macroporous zeolite HY

DOI: 10.1134/S0965544120080034

Benzyl alkyl ethers hold an important position in the class of ethers. Benzyl methyl and benzyl butyl ethers characterized by a pleasant fruity odor are commonly used in actual practice. Of all benzyl alkyl ethers, benzyl butyl ether is most in demand and, having a low toxicity, it is used to flavor food products (drinks, pastry, ice cream), perfumes, and cosmetics [1].Benzyl alkyl ethers can be synthesized by several methods. The most selective method to synthesize these ethers is the Williamson ether synthesis, which is based on the reaction of alkali metal alcoholates with benzyl halides [2–4] or the reaction of benzyl alcohol with alkyl halides in the presence of bases and phase transfer catalysts [5, 6].There are published data on the efficient synthesis of benzyl alkyl ethers in the presence of metal complex catalysts [7]. Thus, Tsai et al. [8] synthesized benzyl methyl ether with a yield of 20% by the $TiCl_4$-activated (0.3 equiv) reaction of benzyl alcohol with methanol. A similar reaction is implemented using transition metal complexes, such as rhenium [$ReBr(CO)_5$] [9] and iridium $IrCl_2Cp^*(NHC)$ [10]. Disadvantages of metal complex catalysts are a low selectivity, which is due to the formation of all three possible ethers (dialkyl, dibenzyl, and benzylalkyl); a low water stability; a high cost; and the impossibility of reusing.

It is known that heterogeneous catalysis has a number of advantages over homogeneous catalysis, namely, a low catalyst consumption; reusability; a long lifetime; the absence of necessity to extract the catalyst from solution, because it is readily separated from the reaction mixture; and a decrease in the amount of waste.

Zeolites have a developed microporous structure and contain Brønsted acid sites; therefore, they attract considerable attention as acid catalysts and their supports [11]. Particular attention has recently been paid to zeolite materials with a hierarchical pore structure, which, owing to the presence of meso- and macropores, provide a better diffusion of reactants and products; this feature provides a higher activity, selectivity, and time-on-stream stability of catalyst systems based on these materials. In addition, the presence of pores of different sizes in these zeolites can affect the selectivity of complex reactions and facilitate the formation of one of the possible isomers depending on the molecule size and the ease of diffusion of the reactants [12].

It has been found in [13–15] that zeolites can catalyze the intermolecular dehydration of alcohols to form ethers. Previously, it was shown that $CuBr_2$ in solution catalyzes the intermolecular dehydration of benzyl and *n*-butyl alcohols to form benzyl butyl ether. Reaction in the presence of $CuBr_2$ (1 mol %) occurs with a high conversion and selectivity for benzyl butyl ether (yield of 91%) [16, 17]. However, this approach is inappropriate for implementation in actual practice because of difficulties in isolating $CuBr_2$-based catalytic complexes and the impossibility of reusing them. It was assumed that the reaction selectivity and the catalyst lifetime can be increased by using copper(II) bromide supported on zeolite HY with a hierarchical pore structure as the catalyst.

The aim of this study was to develop a selective and commercially promising method for synthesizing benzyl butyl ether by the intermolecular dehydration of benzyl and *n*-butyl alcohols over a novel heterogeneous catalyst based on $CuBr_2$ supported on zeolite HY with a hierarchical pore structure.

EXPERIMENTAL

Materials and Reagents

The precursors were *n*-butyl alcohol (Bu^nOH, 99%), benzyl alcohol (BnOH, 99%), and $CuBr_2$ (99%), all available from Acros Organics.

Synthesis Procedure for Supported $CuBr_2$/HY Catalyst System

Zeolite HY with a micro–meso–macroporous structure was used as a support; the zeolite synthesis is described in [18]; hereinafter, it is referred to as HY. Supported $CuBr_2$/HY catalysts were prepared by the incipient wetness impregnation of a calcined pelletized HY zeolite with a $CuBr_2$ alcoholic solution to synthesize catalysts with a given salt content. After impregnation, the pellets were dried in a nitrogen atmosphere at 170°C to remove alcohol and adsorbed water. Samples with a salt content of 5, 10, and 20 wt % are designated as $CuBr_2$(5%)/HY, $CuBr_2$(10%)/HY, and $CuBr_2$(20%)/HY, respectively.

Catalytic Testing Procedures

The intermolecular dehydration of benzyl and butyl alcohols was run in a flow reactor at 140–160°C and a pressure of 1 atm with a catalyst load of 2 g (fractional composition of 0.1–0.2 mm). The BnOH : Bu^nOH molar ratio in the feedstock was 1 : 4. The feed space velocity was $1.0\ h^{-1}$. Before the reaction, the catalyst was preheated at 170°C in a dry nitrogen stream (3 mL/min) for 3 h to remove adsorbed moisture. Reaction products were sampled at intervals of 4 h.

Analysis Methods

Copper(II) bromide content in the dried catalyst samples was determined by X-ray fluorescence spectrometry on a Shimadzu EDX 900HS instrument.

X-ray diffraction (XRD) analysis of the uncalcined samples was conducted on a Bruker D8 Advance diffractometer using CuK_α radiation. Scanning was conducted in a 2θ angular range of 3° to 50°–80° with a step size of 1°/min; the acquisition time was 2 s per point. The XRD patterns were processed using the TOPAS and EVA software programs and the PDF2 database.

Specific surface area and micro- and mesopore volumes were determined by low-temperature nitrogen adsorption–desorption on a Nova 1200e sorption meter. The specific surface area was calculated by the Brunauer–Emmett–Teller (BET) method for a relative partial pressure of $P/P_0 = 0.2$ [19].

Macropore volume was determined by mercury porosimetry on a Porosimeter-2000 instrument. Mercury penetration into pores with a radius of 30–10000 Å was performed at a pressure of 0.1–200 MPa.

To determine the valence state of copper in the catalyst composition, electronic diffuse reflectance spectra of samples in the ultraviolet and visible regions were recorded on a Shimadzu UV-2501 PC spectrometer in a spectral range of 200–900 nm using an IRS-250A diffuse reflectance attachment. The spectra of the catalyst samples were recorded in air without preconditioning. Prior to spectra recording, the powdered catalysts were placed in a quartz cell with an optical path length of 2 mm. The experimentally determined radiation reflection coefficients (*R*) were converted to units of the Kubelka–Munk function *F*(*R*) by the following equation: $F(R) = (1 - R)^2/2R$.

Chromatographic analysis of the products was conducted on a Shimadzu GC-9A instrument (2 m × 3 mm column; stationary phase, SE-30 (5%) on Chromaton N-AW-HMDS; temperature programming, 50–270°C; heating rate, 8°C/min; carrier gas, helium (47 mL/min)).

Mass spectra were recorded on a Shimadzu GCMS-QP2010Plus gas chromatograph–mass spectrometer system (30 m × 0.25 mm SPB-5 capillary column; carrier gas, helium, temperature programming, 40–300°C; heating rate, 8°C/min; evaporator temperature, 280°C; ion source temperature, 200°C; ionization energy, 70 eV).

Nuclear magnetic resonance (NMR) spectra were recorded on Bruker Avance-400 spectrometers (400.13 and 100.62 MHz, respectively) in $CDCl_3$.

RESULTS AND DISCUSSION

Table 1 shows results of elemental analysis for dried catalyst samples. It is evident that the $CuBr_2$ content in the catalyst is close to the calculated value.

Figure 1 shows XRD patterns of the studied samples. It is evident that the XRD patterns for all the samples exhibit the principal signals characteristic of a HY zeolite phase with high phase purity and crystallinity. For the sample with a $CuBr_2$ content of 20%, there is a signal at 45°, which is attributed to the presence of the $CuBr_2$ phase. The absence of this signal for the samples with a lower salt content is apparently due to the high degree of dispersion of the $CuBr_2$ particles. It should be noted that the introduction of $CuBr_2$ into the zeolite composition has hardly any effect on the phase composition and crystallinity of the zeolite; this fact suggests that the structure of the selected zeolite is stable with respect to the introduction of the active component.

Table 2 lists characteristics of the pore structure of the studied samples. The data show that the HY zeolite

Table 1. Chemical and phase composition of the catalysts

Sample	Chemical composition	Phase composition
HY	$Al_{1.00}Si_{3.02}$	FAU
$CuBr_2$(5%)/HY	$Cu_{0.11}Br_{0.18}\ Al_{1.00}Si_{3.10}$	FAU
$CuBr_2$(10%)/HY	$Cu_{0.19}Br_{0.39}\ Al_{1.00}Si_{3.09}$	FAU
$CuBr_2$(20%)/HY	$Cu_{0.42}Br_{0.80}\ Al_{1.00}Si_{3.11}$	FAU + $CuBr_2$

sample has a micro–meso–macroporous structure. It is evident that an increase in the $CuBr_2$ content in the catalyst leads to a decrease in the specific surface area and the micropore and mesopore volume; this finding is attributed to the partial filling of the inner space of the pores with copper(II) bromide. It should be noted that the macropore volume remains almost unchanged; this fact is apparently associated with the dominant localization of copper bromide in micro- and mesopores.

To determine the valence state of copper in the catalyst, diffuse reflectance electronic spectra of the samples in the ultraviolet and visible regions were recorded. Figure 2 shows the spectra of the catalyst samples. It is evident that the spectrum of the $CuBr_2$-containing samples exhibits two absorption maxima at a wavelength of ~336 nm [20] and ~900 nm [21, 22], which are characteristic of $CuBr_2$. The data suggest that copper is present mostly in the form of bromide ($CuBr_2$). With an increase in the $CuBr_2$ content, the intensity of these bands increases; it is in good agreement with the increase in the copper loading of the catalyst samples.

It was previously shown [16, 17] that the reaction of *n*-butyl and benzyl alcohols in the presence of $CuBr_2$ as a catalyst leads to the formation of benzyl butyl ether and byproducts, namely, dibutyl and dibenzyl ethers (Scheme 1).

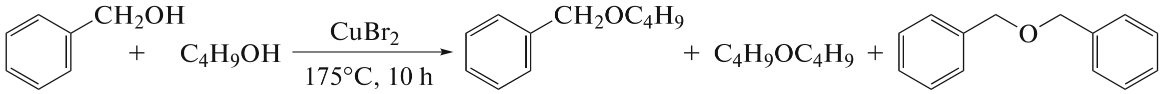

Scheme 1.

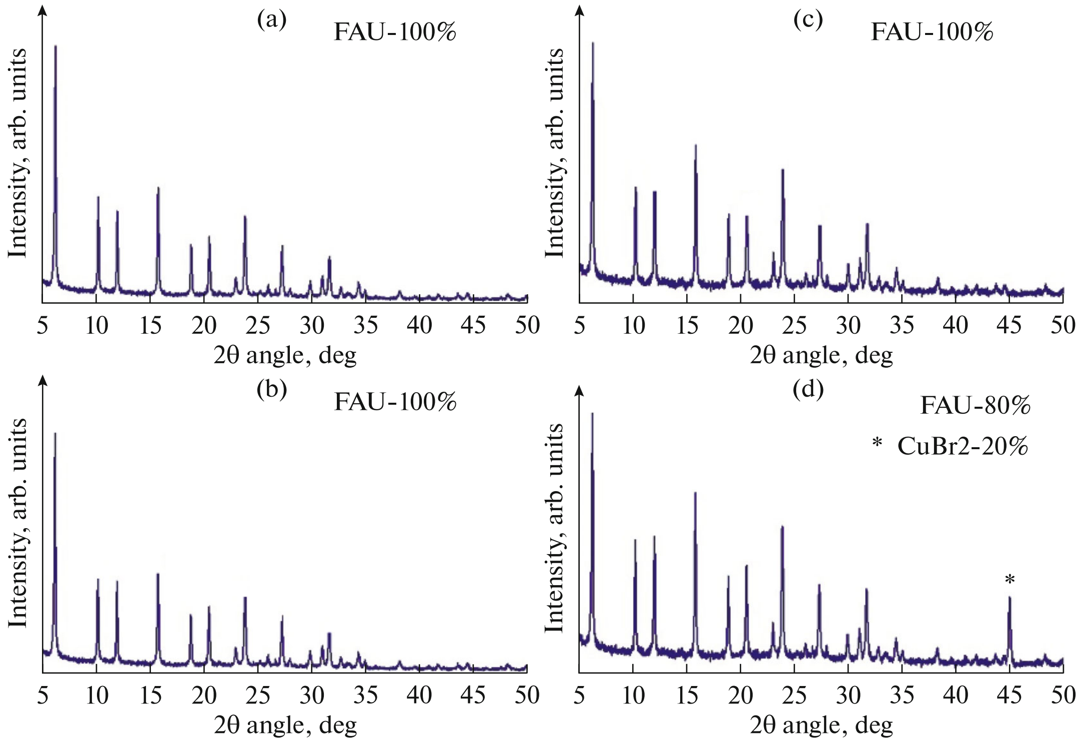

Fig. 1. X-ray diffraction patterns of catalyst samples: (a) zeolite HY, (b) $CuBr_2$(5%)/HY, (c) $CuBr_2$(10%)/HY, and (d) $CuBr_2$(20%)/HY.

Table 2. Characteristics of the pore structure of the samples

Sample	S_{BET}, m^2/g*	V_{micro}, cm^3/g**	V_{meso}, cm^3/g***	V_{macro}, cm^3/g****
HY	735	0.28	0.15	0.15
$CuBr_2$(5%)/HY	701	0.21	0.11	0.15
$CuBr_2$(10%)/HY	360	0.11	0.10	0.15
$CuBr_2$(20%)/HY	120	0.04	0.08	0.15

* Specific surface area determined by the BET method.
** Specific micropore volume.
*** Specific mesopore volume.
**** Specific macropore volume.

Table 3. Benzyl butyl ether synthesis by reaction between benzyl and butyl alcohols in the presence of heterogeneous catalysts

Sample	BnOH conversion, %	BnOBu selectivity, %	BnOBn selectivity, %	BnOBu yield, %
HY	4	75	25	3
$CuBr_2$(5%)/HY	59	76	24	45
$CuBr_2$(10%)/HY	100	95	5	95
$CuBr_2$(20%)/HY	60	83	17	50

Reaction conditions: 150°C; space velocity, 1 h^{-1}; and catalyst time on stream, 8 h.
Legend: BnOH, benzyl alcohol; BnOBu, benzyl butyl ether; and BnOBn, dibenzyl ether.

In this paper, we describe the results of this reaction in the presence of the heterogeneous catalysts zeolite HY and $CuBr_2$/HY (Table 3). It is evident that zeolite HY without a $CuBr_2$ additive exhibited low activity in benzyl butyl ether synthesis. Thus, at 150°C, the benzyl alcohol conversion does not exceed 4% at a benzyl butyl ether selectivity of ~75%. The introduction of $CuBr_2$ into the zeolite composition provides a significant increase in the benzyl alcohol conversion and the benzyl butyl ether selectivity. The best result was obtained in the case of using the $CuBr_2$(10%)/HY catalyst sample, for which the benzyl alcohol conversion was 100% and the ether selectivity was 95%. The dibutyl ether yield does not exceed 1% in all the tests. It should be noted that a further increase in the $CuBr_2$ content in the catalyst leads to a decrease in the catalyst activity. This result can be attributed to the decrease in the degree of dispersion of $CuBr_2$ in the catalyst composition and the formation of an individual $CuBr_2$ phase; this assumption is confirmed by the XRD and nitrogen adsorption results.

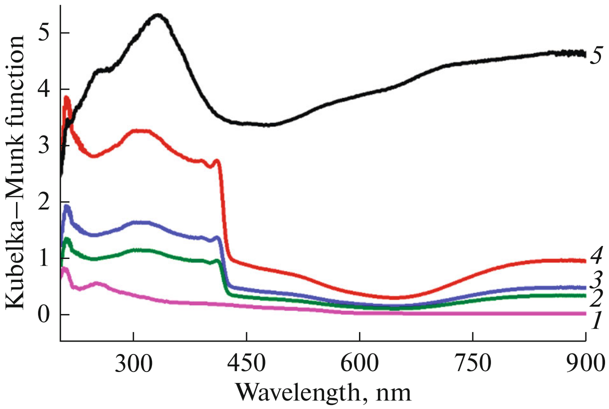

Fig. 2. Ultraviolet diffuse reflectance spectra of catalyst samples: (*1*) zeolite HY; (*2*) $CuBr_2$(5%)/HY, (*3*) $CuBr_2$(10%)/HY, (*4*) $CuBr_2$(20%)/HY, and (*5*) $CuBr_2$.

To verify the catalyst time-on-stream stability and reusability, repeated tests at a catalyst on-stream time of 1–48 h were conducted (Fig. 3).

It is evident from Fig. 3 that the $CuBr_2$(10%)/HY catalyst retains active and highly selective in the intermolecular dehydration of benzyl and *n*-butyl alcohols to benzyl butyl ether for 48 h.

Thus, a highly efficient and selective catalyst based on copper(II) bromide supported on a micro–macro–mesoporous HY zeolite, which facilitates the intermolecular dehydration of benzyl and *n*-butyl alcohols to selectively form benzyl butyl ether with a yield of ~95%, has been developed. It has been shown that the catalyst remains active in a flow unit without loss of activity and benzyl butyl ether selectivity for 48 h.

ACKNOWLEDGMENTS

This work was performed using the equipment of the “Agidel” Shared-Use at the Ufa Federal Research Center of the Russian Academy of Sciences.

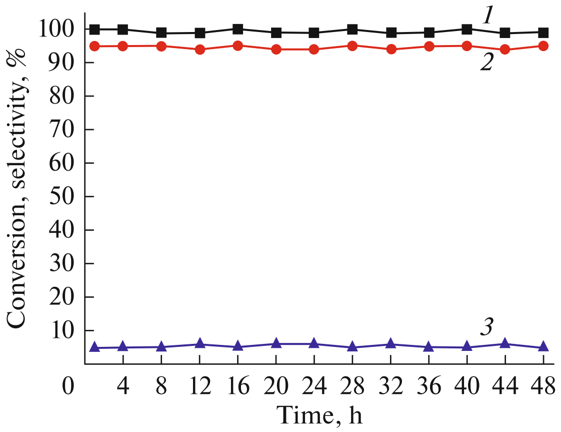

Fig. 3. Data on the on-stream stability of the $CuBr_2$(10%)/HY catalyst sample in benzyl butyl ether synthesis by the intermolecular dehydration of benzyl alcohol with *n*-butyl alcohol: (*1*) benzyl alcohol conversion, (*2*) benzyl butyl ether selectivity, and (*3*) dibutyl ether selectivity.

FUNDING

This work was supported by the Ministry of Education and Science of the Russian Federation (Federal target program project no. 2019-05-595-000-058) and the Russian Foundation for Basic Research (project no. 17-43-020155r_a) and performed under a state task (state registration no. AAAA-A19-119022290009-3).

REFERENCES

1. G. A. Burdock, *Fenaroli's Handbook of Flavor Ingredients*, 6th Ed. (CRC, Boca Raton, 2016), p. 146.
2. O. Sirkecioglu, B. Karliga, and N. Talinli, Tetrahedron Lett. **44**, 8483 (2003).
3. G. Jin, T. Ido, and S. Goto, Catal. Today **64**, 279 (2001).
4. G. Jin, C. Zhang, T. Ido, and S. Goto, Catal. Lett. **98**, 107 (2004).
5. S. T. A. Shah, K. M. Khan, H. Hussain, et al., Tetrahedron **61**, 6652 (2005).
6. M. Motoi, K. Shimamura, C. Shimamura, et al., Bull. Chem. Soc. Jpn. **62**, 2553 (1989).
7. R. I. Khusnutdinov and A. R. Bayguzina, Russ. J. Org. Chem. **55**, 903 (2019).
8. C.-Y. Tsai, R. Sung, B.-R. Zhuang, and K. Sung, Tetrahedron **66**, 6869 (2010); Y. Liu, R. Hua, H.-B. Sun, and X. Qiu, Organometallics **24**, 2819 (2005).
9. A. Prades, R. Corberan, M. Poyatos, and E. Peris, Chem.-Eur. J. **14**, 11474 (2008).
10. A. Klerk, Molecules **23**, 115 (2018). https://doi.org/10.3390/molecules23010115
11. M. Hartmann, A. G. Machoke, and W. Schwieger, Chem. Soc. Rev. **45**, 3313 (2016). https://doi.org/10.1039/c5cs00935a
12. A. Wali and S. M. Pillai, J. Chem. Res. (S), No. 5, 326 (1999). doi org/ https://doi.org/10.1039/A807189F
13. T. Mitsudome, T. Matsuno, S. Sueoka, et al., Green Chem. **14**, 610 (2012). https://doi.org/10.1039/c2gc16135d
14. M. A. Makarova, E. A. Paukshtis, J. M. Thomas, et al., J. Catal. **149**, 36 (1994). doi org/ https://doi.org/10.1006/jcat.1994.1270
15. A. R. Bayguzina, L. I. Gimaletdinova, and R. I. Khusnutdinov, Russ. J. Org. Chem. **54**, 1148 (2018). https://doi.org/10.1134/S1070428018080055
16. U. M. Dzhemilev, R. I. Khusnutdinov, A. R. Bayguzina, and L. I. Gimaletdinova, RU Patent No. 2536486 (2014).
17. O. S. Travkina, M. R. Agliullin, N. A. Filippova, et al., RSC Adv. **7**, 32581 (2017). https://doi.org/10.1039/C7RA04742H
18. S. J. Gregg, K. S. W. Sing, and H. W. Salzberg, J. Electrochem. Soc. **114**, 279 (1967). https://doi.org/10.1149/1.2426447
19. H. Hajifatheali, E. Ahmadi, A. Wojtczak, and Z. Jaglicic, Macromol. Res. **23**, 977 (2015). https://doi.org/10.1007/s13233-015-3132-z
20. S. Firlik, W. Skupiński, Z. Wielgosz, and J. Stasiński, Polimery **60**, 372 (2015). https://doi.org/10.14314/polimery.2015.372
21. J. J. N. Segoviano-Garfias, R. Moreno-Esparza, and G. Mendoza-Diaz, Inorg. Chim. Acta **363**, 3461 (2010). https://doi.org/10.1016/j.ica.2010.06.050

Translated by M. Timoshinina